
Article:
Lamberto, G., Amin, D., Solomon, L.B. et al. (2019) Personalised 3D knee compliance from clinically viable knee laxity measurements: A proof of concept ex vivo experiment. Medical Engineering and Physics, 64. pp. 80-85. ISSN: 1350-4533

https://doi.org/10.1016/j.medengphy.2018.12.003

PERSONALISED 3D KNEE COMPLIANCE FROM CLINICALLY VIABLE KNEE LAXITY MEASUREMENTS: A PROOF OF CONCEPT *EX VIVO* EXPERIMENT

[1,2]Giuliano Lamberto, [3]Dhara Amin, [4,5]Lucian Bogdan Solomon, [6]Boyin Ding, [3]Karen J Reynolds, [1,2]Claudia Mazzà, and [3]Saulo Martelli

[1]Department of Mechanical Engineering, University of Sheffield, United Kingdom

[2]INSIGNEO Institute for *in silico* Medicine, University of Sheffield, United Kingdom

[3]Medical Device Research Institute, College of Science and Engineering, Flinders University, Adelaide, SA, Australia

[4]Centre for Orthopaedic and Trauma Research, the University of Adelaide, Adelaide, SA, Australia

[5]Department of Orthopaedics and Trauma, Royal Adelaide Hospital, Adelaide, SA, Australia

[5]School of Mechanical Engineering, University of Adelaide, Adelaide, SA 5005, Australia

Type of manuscript: Technical Note

Word count. Abstract: 249; Manuscript (introduction to discussion): 2306

Corresponding Author:

Dr Saulo Martelli
Medical Device Research Institute
College of Science and Engineering
Flinders University
Tonsley SA
Australia
E-mail: saulo.martelli@flinders.edu.au

Keywords: Knee stiffness; compliance matrix; laxity; clinical tests, ligament injury.

Abstract

Personalised information of knee mechanics is increasingly used for guiding knee reconstruction surgery. We explored use of uniaxial knee laxity tests mimicking Lachman and Pivot-shift tests for quantifying 3D knee compliance in healthy and injured knees. Two heathy knee specimens (males, 60 and 88 years of age) were tested. Six-degree-of-freedom tibiofemoral displacements were applied to each specimen at 5 intermediate angles between 0° and 90° knee flexion. The force response was recorded. Six-degree-of-freedom and uniaxial tests were repeated after sequential resection of the anterior cruciate, posterior cruciate and lateral collateral ligament. 3D knee compliance (C_{6DOF}) was calculated using the six-degrees-of-freedom measurements for both the healthy and ligament-deficient knees and validated using a leave-one-out cross-validation. 3D knee compliance (C_{CT}) was also calculated using uniaxial measurements for Lachman and Pivot-shift tests both conjointly and separately. C_{6DOF} and C_{CT} matrices were compared component-by-component and using principal axes decomposition. Bland-Altman plots, median and 40^{th}-60^{th} percentile range were used as measurements of bias and dispersion. The error on tibiofemoral displacements predicted using C_{6DOF} was < 9.6 % for every loading direction and after release of each ligament. Overall, there was good agreement between C_{6DOF} and C_{CT} components for both the component-by-component and principal component comparison. The dispersion of principal components (compliance coefficients, positions and pitches) based on both uniaxial tests was lower than that based on single uniaxial tests. Uniaxial tests may provide personalised information of 3D knee compliance.

1 Introduction

Knee reconstruction surgery postoperative outcome is determined by a variety of surgery variables and their interaction specific to each patient [1]. As such, personalised models of knee mechanics are increasingly used for pre- and post-surgical assessment of knee function and for guiding the intra-operative decision-making in knee replacement and ligament reconstruction surgery [2]. For example, personalized models based on the healthy knee can be used to restore loading patterns in passive restraints in the contra-lateral injured knee whereas personalized models of the injured knee may inform the decision process for proper management of knee injuries. However, generating personalised models is complex as it requires combining information of subject's anatomy from medical images [3,4], knee motion and material properties [5] or performing complex six-degree-of-freedom (6DOF) tests for determining 3D knee compliance [6,7]. In this study, we explore the use of two different uniaxial knee laxity tests for determining the 3D knee compliance in healthy and injured knees.

Personalised knee models can provide the contribution to knee function of each knee structure. For example, *ex vivo* knee laxity measurements have been used to calibrate ligament stiffness in models of native [8] and artificial knees [9]. Some authors combined personalised knee anatomy from Magnetic Resonance Images and ex vivo knee laxity measurements [3,4] while others modelled knee mechanics of knee specimens using both imaging and complex in vitro experiments [2,5]. In a previous study by Lamberto et al. [6] we have developed a protocol for measuring *ex vivo* the 3D knee compliance matrix of the tibiofemoral joint and demonstrated the feasibility of embedding 3D knee compliance in models of human motion for studying knee mechanics in vivo [7]. However, determination of

79 3D knee compliance requires complex experimental protocols that are impractical in the
80 clinic [6].

81 Arthrometers are clinically viable solutions for providing objective measurements of
82 knee laxity along a single direction of movement [1,10,11]. For example, the integrity of the
83 anterior cruciate ligament (ACL) can be assessed using measurements of tibiofemoral motion
84 while applying an anterior tibial force of 134 N at 20° – 30° knee flexion (Lachman test,
85 [12]). The Pivot-shift test provides both information of ACL integrity and general knee
86 stability by applying to the knee a medial force while the knee is kept 30° – 40° flexed and
87 20° internally rotated [13]. Establishing a relationship between clinical knee laxity tests (e.g.,
88 Lachman and Pivot-shift) and 3D knee compliance requires to first establish the relationship
89 between the two uniaxial measurements and the 3D knee compliance matrix and then to
90 assess the tools that could be used to obtain the measurements required when in the clinics.
91 Here, we tackled the first step and hypothesised that in vitro measurements of knee
92 compliance obtained using simple uniaxial tests mimicking Lachman and Pivot-shift tests can
93 be used to determine, conjointly or in isolation, the 3D knee compliance in healthy and
94 injured knees.

95 The aim of this study was to calculate and compare 3D knee compliance using full
96 6DOF and uniaxial experiments mimicking Lachman and Pivot-Shift tests in healthy and
97 ligament-deficient knees. We developed a protocol for measuring 3D knee compliance using
98 the hexapod robot by Ding et al. [14]. 3D knee compliance matrices based on full 6DOF
99 experiments were calculated, validated using leave-one-out cross validation, and compared to
100 corresponding matrices based on uniaxial experiments using bias and dispersion indicators.

101 **Materials and Methods**

Experimental procedure

Two fresh-frozen right knees from two male donors (age at death: 60 and 88; body weight: 91 kg for both donors; height: 178 and 183 cm) were obtained from a body donation program (Science Care, Phoenix, USA). Ethics clearance was obtained from the institutional Ethics Committee at Flinders University. Ligaments, cartilage and menisci were found intact on MRI inspection [15] and surgical inspection.

Specimens were thawed 24 hours at room temperature. Tibia, fibula and femur were cut at mid shaft and soft tissues removed 15 cm above and below the femoral epicondyles. Tibiofemoral joint coordinate system was defined according to the work of Grood and Suntay [16], assuming coincident tibial and femoral coordinate systems at full knee extension. The tibia was cemented in an aluminium cup by aligning the tibial plateau to the cup's base. Tibia and fibula were rigidly fixed using a cortical screw. The femur was fixed to the specimen holder using a transfix pin through the femoral diaphysis and four cortical screws.

The femur's specimen holder was mounted on the hexapod robot (Figure 1) through a screw mechanism. The vertical distance between the bottom and top plate, the knee centre (midpoint between medial and lateral femoral epicondyles) and the x-, y- and z- offset were used for mounting the knee specimen, ensuring alignment of knee and hexapod robot coordinate systems. Two different reference configurations were defined using an auxiliary device (Figure 2) for testing the specimens over 90° knee flexion despite the relatively small range of motion of the hexapod robot (approximately ± 25°). Firstly, the knee specimen flexed at 15° was fixed on the hexapod device, ensuring the knee sagittal plane and trans-epicondylar axis were aligned to the device planes and tested at 0°, 15°, 30° knee flexion angle. Secondly, the knee was flexed at 75° was similarly fixed to the hexapod device and tested at 60° and 90° knee flexion angle (Figure 2).

126 The force response to controlled tibiofemoral displacement and rotation (position-
127 control) about each of the six axes was measured. The neutral tibiofemoral position at each
128 knee flexion angle was determined by defining the knee flexion path offering minimal
129 resistance using a hybrid control algorithm built-in the hexapod control system [14]. Positive
130 and negative displacements and rotations were applied from the neutral tibiofemoral position
131 at 0.33 mm/s and 0.33°/s, respectively. Axial translations were run at 0.10 mm/s. The
132 displacement direction was reversed when knee stiffness, displacement and load exceeded,
133 respectively, 20% increase from linear force response, ±10 mm medial and anterior
134 displacement, ±5 mm proximal displacement, ±10° rotation, 200 N and 20 Nm.

135 The force-control tests mimicked the uniaxial Lachman [17] and Pivot-Shift tests [13]
136 using an adaptive velocity-based load control algorithm [18]. An anterior tibial force of ±100
137 N was used for mimicking the Lachman test. A ±10 Nm moment about the abduction and
138 internal rotation axis was applied to mimic the Pivot-Shift test.

139 Position-control (6DOF) and uniaxial force-control experiments were repeated after
140 sequential resection of anterior cruciate, posterior cruciate and lateral collateral ligaments by
141 a single experienced orthopaedic surgeon. Anterior and posterior cruciate ligaments were
142 released through an anterior incision and patella tendon split (Figure 1c) while the final
143 release of the lateral collateral ligament was completed through a lateral incision. Each
144 incision was sutured after resection. The force threshold causing the displacement direction to
145 reverse for the 6DOF tests was reduced by 10% – 20% after each resection.

146 The compliance matrix

147 The compliance matrix C_{6DOF} was determined using position-control measurements
148 and an earlier work [6]. Displacement and load matrices were:

$$[\Delta X] = [X - X_0] = [X_{medial}^{+/-}\ X_{anterior}^{+/-}\ X_{axial}^{+/-}\ X_{adduction}^{+/-}\ X_{internal}^{+/-}\ ] \quad (1)$$

$$[\Delta F] = [F - F_0] = [F_{medial}^{+/-}\ F_{anterior}^{+/-}\ F_{axial}^{+/-}\ F_{adduction}^{+/-}\ F_{internal}^{+/-}] \quad (2)$$

where X_0 and F_0 represent the generalised displacement and force vector for each test; $X_i^{+/-}$ contains linear and angular displacements in the joint coordinate systems; $F_i^{+/-}$ contains the forces and moments. The coefficient of determination was calculated for studying the linearity of the force-displacement relationship. The compliance matrix was calculated (Matlab, The MathWorks, USA) by minimizing the difference between measured and predicted displacements. The objective function J(C) was formulated as:

$$\mathrm{J(C)} = \|[\mathrm{C}_{6DOF}][\Delta F] - [\Delta X]\|_{mm} + w \cdot \|[\mathrm{C}_{6DOF}][\Delta F] - [\Delta X]\|_{rad} \quad (3)$$

where the first term represents the norm of the error on translational components and the second term represents the norm of error on rotational components. The weight *w* was used for evenly weight translational and rotational errors and assumed equal to the femoral inter-epicondyles distance. The compliance matrix C_{ct} was similarly calculated using the Lachman and Pivot-shift tests conjointly and separately. C_{ct} and C_{6DOF} matrices were also decomposed using principal axis decomposition, thus providing an equivalent system of two orthogonal sets of three torsional and three screw springs defined by compliance coefficients, position, pitches and directions [19].

The model accuracy was quantified using a leave-one-out cross-validation. Datasets of ΔX and ΔF were randomly divided in five groups, four for training and one for validation. Components in the original C_{ct} and C_{6DOF} matrices were grouped into translational, rotational and coupled movements components. Components in the decomposed matrices were grouped into compliance coefficients, directions, positions and pitches.

Tibiofemoral translations and rotations were predicted using C_{6DOF} matrices. The error was calculated as the difference between predicted ($D_{predicted}$) and measured tibiofemoral displacement ($D_{measured}$). The root mean square error was calculated and normalized by the displacement range:

$$NRMSE = \frac{RMSE(D_{predicted} - D_{measured})}{Dmax - Dmin} * 100 \quad (4)$$

The NRMSE's mean and standard deviation were calculated for each specimen and test.

Bland-Altman plots, median and 40^{th} – 60^{th} percentile range were used as measures of bias and dispersion for comparing C_{ct} and C_{6DOF} matrices.

2 Results

The coefficient of determination calculated from the recorded force and displacement was systematically above 0.9. The tibiofemoral displacement error committed by matrix C_{6DOF} was below 9.6% for each specimen, ligaments' integrity and loading direction. The normalised error was NRMSE = 9.6% ± 1.9% for translations and NRMSE = 6.1% ± 0.7% for rotations in one specimen and NRMSE = 8.4% ± 1.6% (translations) and NRMSE = 6.7% ± 1.1% (rotations) for the other.

The compliance matrix C_{ct} and C_{6DOF} showed a good component-by-component agreement both in the knee joint space and after principal component decomposition (Figure 3 – 4). In the knee joint space, similar bias and dispersion were found using both uniaxial tests and the Lachman-like test only. The bias was below 0.00473 ± 0.00062 mm\N for translations, 0.00347 ± 0.00099 N^{-1} for rotations and 0.00010 ± 0.00005 $N^{-1}\times mm^{-1}$ for coupled movements. Using the Pivot-shift tests only, bias and dispersion were higher, particularly for translation; the bias (0.01763 mm\N) was more than three times higher than

191 that calculated using both uniaxial tests while dispersion (-0.00523 mm\N) was more than
192 eight times higher than the dispersion calculated using both uniaxial tests. Principal
193 components showed comparable bias and dispersion using Lachman- and Pivot-shift-like
194 tests separately, showing a moderately lower dispersion of the compliance coefficients,
195 positions and pitches but not of directions in the Pivot-Shift test only matrix. A general
196 further reduction of bias and dispersion of compliance coefficients, positions and pitches but,
197 again, not for directions, was observed using both uniaxial tests (Figure 4 and Table 2).

198 **Discussion**

199 We proposed a novel protocol for 6DOF testing of human knees, calculating 3D knee
200 compliance matrices using 6DOF experiments and simpler uniaxial tests mimicking Lachman
201 and Pivot-Shift tests. We found that combined uniaxial tests mimicking Lachman and Pivot-
202 shift tests can best provide information of compliance coefficients, position and pitches along
203 the principal axes of the 3D tibiofemoral compliance matrix, showing higher dispersion of
204 their directions. Therefore, 3D knee compliance can be obtained from a reduced number of
205 accurate uniaxial measurements of knee laxity.

206 The compliance matrix C_{6DOF}, calculated using full 6DOF experiments, predicted
207 tibiofemoral displacements and rotations within 9.6% error for both specimens in intact and
208 ligament-deficient conditions (three ligaments completely resected). Similar results were
209 obtained during earlier work [6] using a serial manipulator, as opposed to the parallel
210 hexapod robot used in the present study, hence providing confidence on the robustness of the
211 method developed here and expanding its validity to multi ligament-deficient knees. There
212 was a good component-by-component agreement between 3D knee compliance based on
213 6DOF and uniaxial experiments (Figure 3 – 4) showing a moderate bias for each studied
214 component. Principal axes decomposition showed lower dispersion of compliance

coefficients, position and pitches, but not directions, when using both uniaxial tests conjointly over that provided by each uniaxial test separately. Therefore, uniaxial tests mimicking Lachman and Pivot-shift tests can provide information of 3D knee compliance. Principal axes decomposition appears to better capture the increased level of information provided by both uniaxial tests over the representation of 3D knee compliance in the knee joint space.

This study has limitations. Firstly, the present study shows that uniaxial tests mimicking Lachman and Pivot-shift tests can be used to determine salient features of the 3D knee compliance in healthy and ligament-deficient knees. Further research is required to determine whether clinically available technologies (e.g., arthrometers) can provide enough information for determining 3D knee compliance and ultimately guiding the clinical management of knee ligament injuries. Secondly, the generality of the present conclusion is limited by only two specimens used, likely resulting in a narrower range of knee compliances than that in human knees. Describing knee compliance in the broader population was outside the purely methodological scope of the present study. Thirdly, the sequential ligament resection performed in the present study may not represent the complex and variable range of possible knee injuries. Here, we showed that the procedure developed is robust to a range of knee health conditions, from intact to ligament-deficient knees. Fourthly, the contribution to 3D tibiofemoral stiffness of the anterior incision and re-suture was not quantified independently from that of ligament resection. However, ligament are the major soft-tissue constraints of tibiofemoral motion and changes of knee stiffness due to the anterior incision and its subsequent suture are likely smaller than changes of knee stiffness due to each ligament resection.

In conclusion, we developed a method for determining 3D knee compliance in healthy and ligament deficient knees using uniaxial tests mimicking common Lachman and Pivot-

shift tests. This may support the development of clinically-viable procedures for the analysis of knee mechanics in specific patients.

Conflicts of Interest:

None.

Funding:

This work was supported by the Government of South Australia; the Australian Research Council (DP180103146; FT180100338); and the UK EPSRC (MultiSim project, EP/K03877X/1).

Ethical Approval:

Ethics clearance was obtained from the institutional Ethics Committee at Flinders University (SBREC 6832).

Acknowledgments

The authors are grateful for the help received during the experiments from Richard Stanley and John Costi (Flinders University). The authors wish to thank Nuruljannah B Mohd Shaffie, David Agban and Scott Robinson (The University of Sheffield) for their help in data processing. Genliang Chen (Shanghai Jiao Tong University) is also gratefully acknowledged for providing assistance and codes for the Principal Axes Decomposition analysis.

References

[1] Kupper JC, Loitz-Ramage B, Corr DT, Hart DA, Ronsky JL. Measuring knee joint laxity: A review of applicable models and the need for new approaches to minimize variability. Clin Biomech 2007;22:1–13. doi:10.1016/j.clinbiomech.2006.08.003.

[2] Kia M, Schafer K, Lipman J, Cross M, Mayman D, Pearle A, et al. A Multibody Knee Model Corroborates Subject-Specific Experimental Measurements of Low Ligament Forces and Kinematic Coupling During Passive Flexion. J Biomech Eng 2016;138:051010. doi:10.1115/1.4032850.

[3] Guess TM, Thiagarajan G, Kia M, Mishra M. A subject specific multibody model of the knee with menisci. Med Eng Phys 2010;32:505–15. doi:10.1016/j.medengphy.2010.02.020.

[4] Guess TM, Liu H, Bhashyam S, Thiagarajan G. A multibody knee model with discrete cartilage prediction of tibio-femoral contact mechanics. Comput Methods Biomech Biomed Engin 2011;16:256–70. doi:10.1080/10255842.2011.617004.

[5] Kiapour A, Kiapour AM, Kaul V, Quatman CE, Wordeman SC, Hewett TE, et al. Finite element model of the knee for investigation of injury mechanisms: development and validation. J Biomech Eng 2014;136:011002. doi:10.1115/1.4025692.

[6] Lamberto G, Richard V, Dumas R, Valentini PP, Pennestrì E, Lu TW, et al. Modeling the human tibio-femoral joint using ex vivo determined compliance matrices. J Biomech Eng 2016;138:In press. doi:10.1115/1.4033480.

[7] Richard V, Lamberto G, Lu T-W, Cappozzo A, Dumas R. Knee Kinematics Estimation Using Multi-Body Optimisation Embedding a Knee Joint Stiffness Matrix: A Feasibility Study. PLoS One 2016;11:e0157010. doi:10.1371/journal.pone.0157010.

[8] Harris MD, Cyr AJ, Ali AA, Fitzpatrick CK, Rullkoetter PJ, Maletsky LP, et al. A Combined Experimental and Computational Approach to Subject-Specific Analysis of Knee Joint Laxity. J Biomech Eng 2016;138:081004. doi:10.1115/1.4033882.

[9] Ewing JA, Kaufman MK, Hutter EE, Granger JF, Beal MD, Piazza SJ, et al. Estimating patient-specific soft-tissue properties in a TKA knee. J Orthop Res 2016;34:435–43. doi:10.1002/jor.23032.

[10] Shultz SJ, Shimokochi Y, Nguyen A-D, Schmitz RJ, Beynnon BD, Perrin DH. Measurement of varus-valgus and internal-external rotational knee laxities in vivo--Part II: relationship with anterior-posterior and general joint laxity in males and females. J Orthop Res 2007;25:989–96. doi:10.1002/jor.20398.

[11] Robert H, Nouveau S, Gageot S, Gagnière B. A new knee arthrometer, the GNRB®: Experience in ACL complete and partial tears. Orthop Traumatol Surg Res 2009;95:171–6. doi:10.1016/j.otsr.2009.03.009.

[12] Lin H-C, Chang C-M, Hsu H-C, Lai W-H, Lu T-W. A new diagnostic approach using regional analysis of anterior knee laxity in patients with anterior cruciate ligament deficiency. Knee Surg Sports Traumatol Arthrosc 2011;19:760–7. doi:10.1007/s00167-010-1354-3.

[13] Kanamori A, Woo SL, Ma CB, Zeminski J, Rudy TW, Li G, et al. The forces in the anterior cruciate ligament and knee kinematics during a simulated pivot shift test: A human cadaveric study using robotic technology. Arthroscopy 2000;16:633–9.

doi:10.1053/jars.2000.7682.

[14] Ding BY, Cazzolato BS, Grainger S, Stanley RM, Costi JJ. Active preload control of a redundantly actuated Stewart platform for backlash prevention. Robot Comput Integr Manuf 2015;32:11–24. doi:DOI 10.1016/j.rcim.2014.09.005.

[15] Dyck P, Smet E, Veryser J, Lambrecht V, Gielen JL, Vanhoenacker FM, et al. Partial tear of the anterior cruciate ligament of the knee: injury patterns on MR imaging. Knee Surgery, Sport Traumatol Arthrosc 2012;20:256–61. doi:10.1007/s00167-011-1617-7.

[16] Grood ES, Suntay WJ. A joint coor dinate system for the clinical description of the three-dimensional motions: application to the knee. J Biomech Eng 1983;105:136–44.

[17] Fujie H, Livesay G, Fujita M, Woo S. Forces and moments in six-DOF at the human knee joint: mathematical description for control. J Biomech 1996;29:1577–85.

[18] Lawless IMM, Ding B, Cazzolato BSS, Costi JJJ. Adaptive velocity-based six degree of freedom load control for real-time unconstrained biomechanical testing. J Biomech 2014;47:3241–7. doi:10.1016/j.jbiomech.2014.06.023.

[19] Chen G, Wang G, Lin Z, Lai X. The Principal Axes Decomposition of Spatial Stiffness Matrices. IEEE Trans Robot 2015;31:1561–4. doi:10.1109/TRO.2015.2496825.

TABLES

Components	Units	Both tests ($\times 10^4$)		Lachman test ($\times 10^4$)		Pivot-shift ($\times 10^4$)	
Translation	mm\N	47.3	(-6.2)	36.7	(2.2)	176.3	(-52.3)
Rotation	N^{-1}	34.7	(9.9)	13.7	(-2.8)	24.8	(-23.2)
Coupling	$N^{-1} \times mm^{-1}$	0.6	(-0.3)	1.0	(-0.5)	1.8	(1)

Table 1 – Bias (median) and dispersion (40^{th} - 60^{th} percentile range) of the component-by-component comparison of C_{CT} and C_{6DOF} .Translational, rotational and coupled components are grouped together. Dispersion is reported in brackets.

Components		Units	Both tests ($\times 10^4$)		Lachman test ($\times 10^4$)		Pivot-shift ($\times 10^4$)	
Compliance coefficients	Screw springs	mm\N	11.5	(-0.2)	19.8	(-7.7)	22.6	(-0.4)
	Torsional springs	N^{-1}	74.1	(14.6)	43.5	(23.3)	217.7	(9.4)
Directions	Screw springs		2035.9	(1117.8)	1359.3	(47.4)	2395.9	(-543.8)
	Torsional springs		2319	(-1204.9)	835.7	(40.4)	1513.1	(-31.3)
Positions		mm	69.8	(-2.2)	131.0	(12.9)	168.4	(24.4)
Pitches		mm	76.8	(10.5)	91.2	(-22)	269.1	(88.9)

Table 2 – Bias (median) and dispersion (40^{th} - 60^{th} percentile range) of C_{CT}'s principal components. Dispersion is reported in brackets.

FIGURE CAPTIONS

Figure 1 – From the left-hand side: (a) frontal view of the hexapod robot and the screw mechanism hosting a dummy femoral and tibial component; (b) detail of one knee specimen mounted on the hexapod robot through the screw mechanism; and (c) the anterior incision used for resecting the cruciate ligaments.

Figure 2 – From the left-hand side: (a) the knee alignment rig assembled with the screw mechanism, (b) the first reference configuration (i.e., 15° knee flexion), and (c) the second reference configuration (i.e., 75° knee flexion).

Figure 3 - Bland-Altman plot for the component-by-component comparison of C_{CT} and C_{6DOF}, reporting the 2.5th and 97.5th percentiles as limits of agreement.

Figure 4 - Bland-Altman plot for the comparison of C_{CT} and C_{6DOF} principal components (CC: Compliance coefficients; S_{Sp}: Screw spring; T_{Sp}: Torsional spring), reporting the 2.5th and 97.5th percentiles as limits of agreement.

TABLES

Components	Units	Both tests ($\times 10^4$)		Lachman test ($\times 10^4$)		Pivot-shift ($\times 10^4$)	
Translation	mm\N	47.3	(-6.2)	36.7	(2.2)	176.3	(-52.3)
Rotation	N^{-1}	34.7	(9.9)	13.7	(-2.8)	24.8	(-23.2)
Coupling	$N^{-1} \times mm^{-1}$	0.6	(-0.3)	1.0	(-0.5)	1.8	(1)

Table 1 – Bias (median) and dispersion (40^{th} - 60^{th} percentile range) of the component-by-component comparison of C_{CT} and C_{6DOF} .Translational, rotational and coupled components are grouped together. Dispersion is reported in brackets.

Components		Units	Both tests ($\times 10^4$)		Lachman test ($\times 10^4$)		Pivot-shift ($\times 10^4$)	
Compliance coefficients	Screw springs	mm\N	11.5	(-0.2)	19.8	(-7.7)	22.6	(-0.4)
	Torsional springs	N^{-1}	74.1	(14.6)	43.5	(23.3)	217.7	(9.4)
Directions	Screw springs		2035.9	(1117.8)	1359.3	(47.4)	2395.9	(-543.8)
	Torsional springs		2319	(-1204.9)	835.7	(40.4)	1513.1	(-31.3)
Positions		mm	69.8	(-2.2)	131.0	(12.9)	168.4	(24.4)
Pitches		mm	76.8	(10.5)	91.2	(-22)	269.1	(88.9)

Table 2 – Bias (median) and dispersion (40^{th} - 60^{th} percentile range) of C_{CT}'s principal components. Dispersion is reported in brackets.

FIGURE CAPTIONS

Figure 1 – From the left-hand side: (a) frontal view of the hexapod robot and the screw mechanism hosting a dummy femoral and tibial component; (b) detail of one knee specimen mounted on the hexapod robot through the screw mechanism; and (c) the anterior incision used for resecting the cruciate ligaments.

Figure 2 – From the left-hand side: (a) the knee alignment rig assembled with the screw mechanism, (b) the first reference configuration (i.e., 15° knee flexion), and (c) the second reference configuration (i.e., 75° knee flexion).

Figure 3 - Bland-Altman plot for the component-by-component comparison of C_{CT} and C_{6DOF}, reporting the 2.5th and 97.5th percentiles as limits of agreement.

Figure 4 - Bland-Altman plot for the comparison of C_{CT} and C_{6DOF} principal components (CC: Compliance coefficients; S_{Sp}: Screw spring; T_{Sp}: Torsional spring), reporting the 2.5th and 97.5th percentiles as limits of agreement.

1 Figure 1

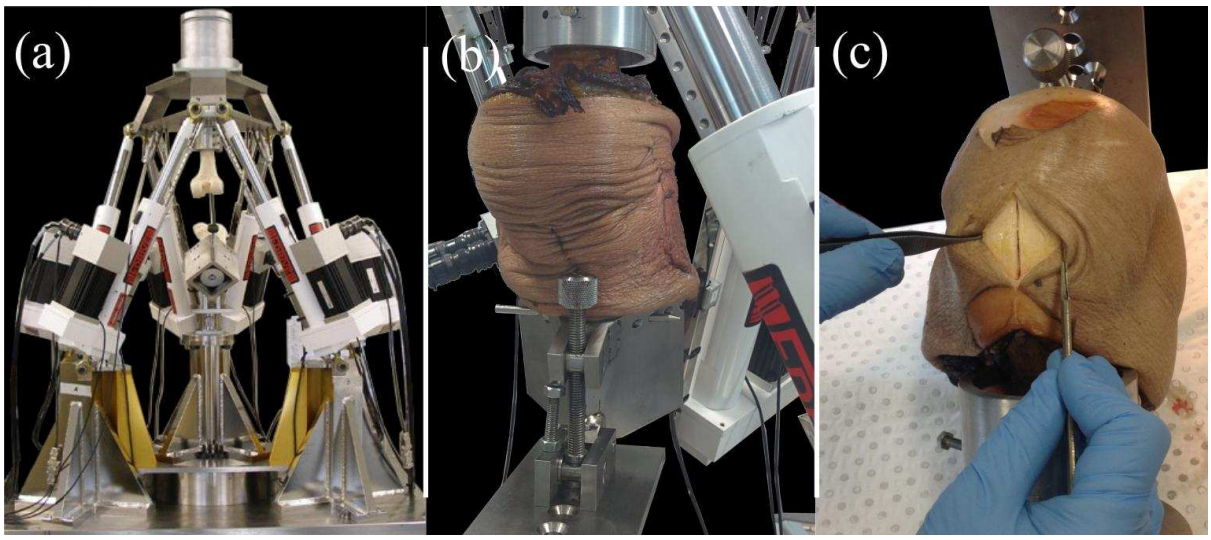

2

3

4 Figure 2

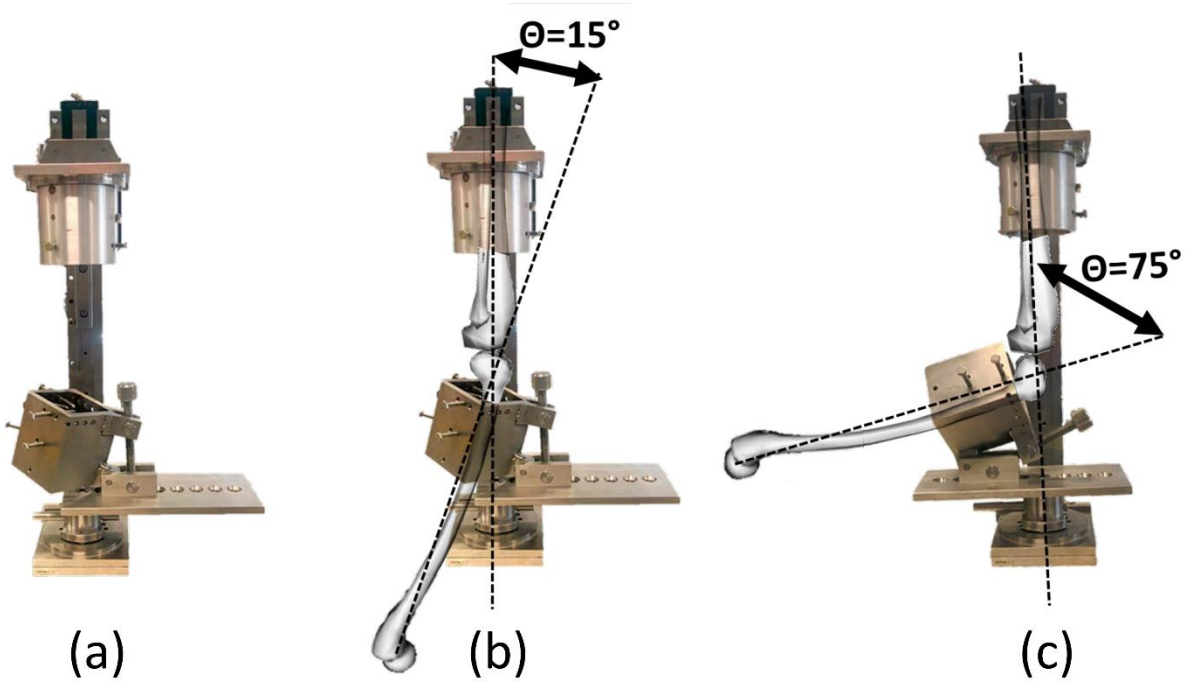

5

6

7 Figure 3

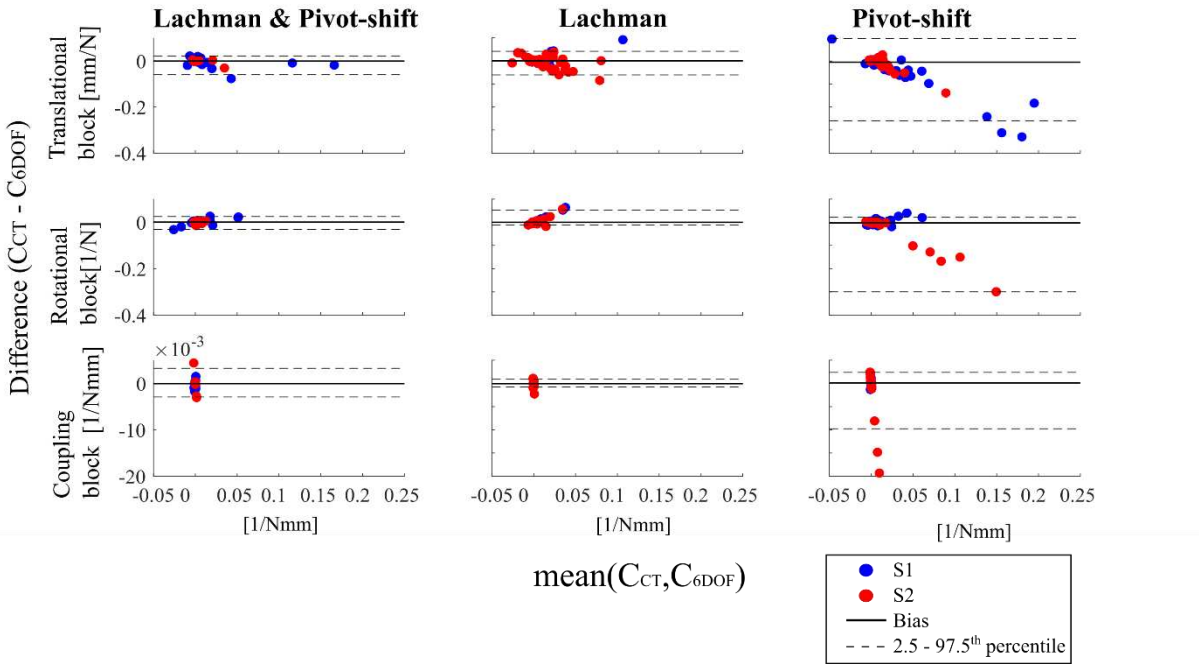
Lachman & Pivot-shift
Lachman
Pivot-shift
Difference (CCT - C6DOF)
Translational block [mm/N]
Rotational block[1/N]
Coupling block [1/Nmm]
×10-3
[1/Nmm]
mean(CCT,C6DOF)
S1
S2
Bias
2.5 - 97.5th percentile

8

9

Figure 4

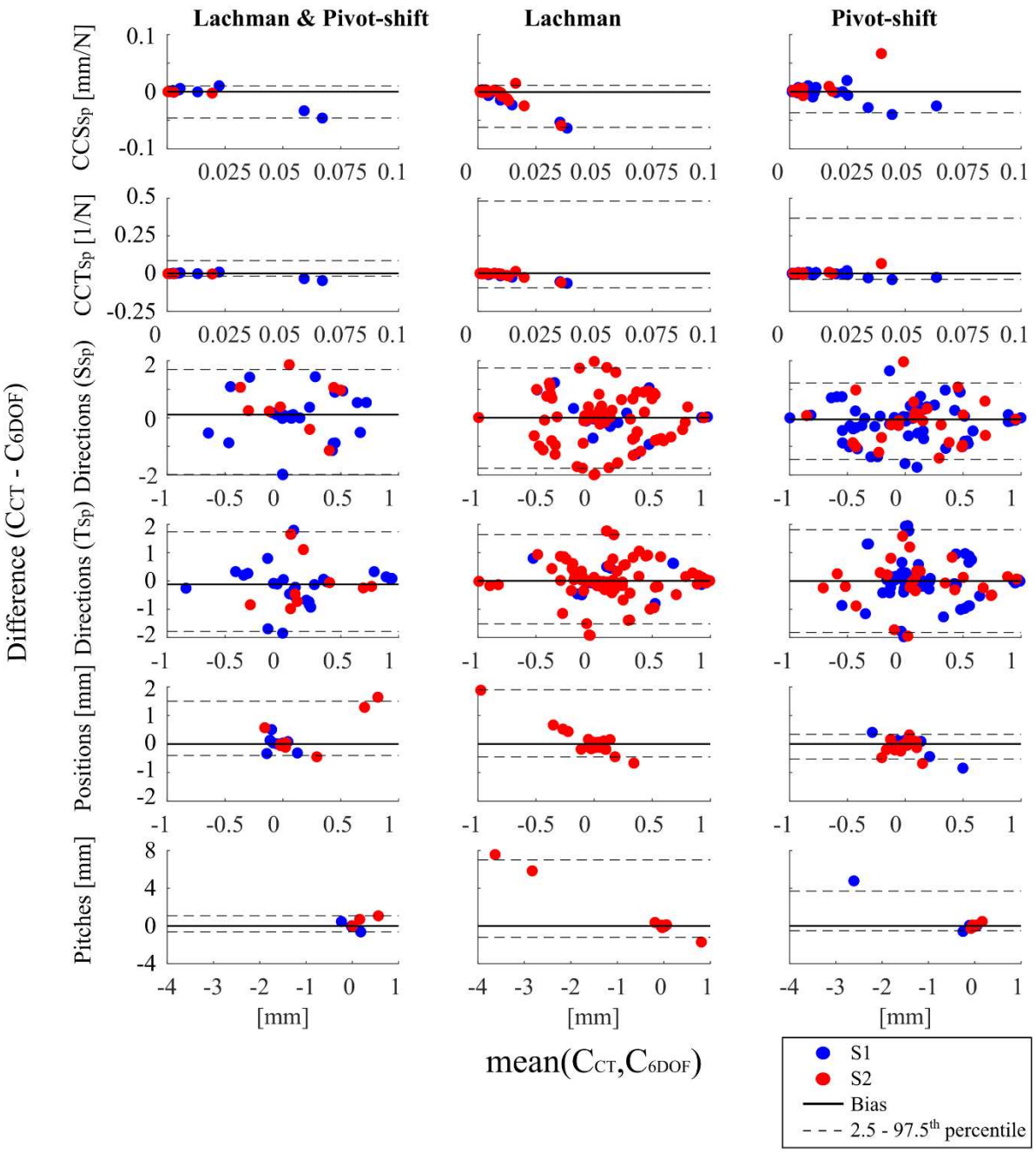
Lachman & Pivot-shift
Lachman
Pivot-shift
Difference (CCT - C6DOF)
CCSSp [mm/N]
CCTSp [1/N]
Directions (SSp)
Directions (TSp)
Positions [mm]
Pitches [mm]
[mm]
mean(CCT,C6DOF)
S1
S2
Bias
2.5 - 97.5th percentile